AIAA JOURNAL
Vol. 36, No. 11, November 1998

Proportional Control of Asymmetric Forebody Vortices

John E. Bernhardt* and David R. Williams†
Illinois Institute of Technology, Chicago, Illinois 60616

The ability of the unsteady bleed technique to control the asymmetry of the steady tip vortices separating from a forebody model is demonstrated. Mean velocity profiles measured behind the forebody model at $\alpha = 45$ deg and $Re = 6.3 \times 10^3$ clearly show the exponential spatial growth of the disturbance in the wake. This exponential growth is consistent with a spatial type of flow instability. The type of spatial instability governing the flow determines the behavior of the vortex system. The continuous variation of vortex position with control input found at $\alpha = 45$ deg is consistent with a convective type of instability and allows proportional control of the forebody vortices with very low forcing amplitudes and input power levels. The forebody wake shows characteristics similar to a global type of instability for the bistable behavior found at $\alpha = 55$ deg. For the global type of flow instability, the vortex system is locked into one of two stable configurations, and proportional control does not seem feasible under these conditions.

Nomenclature

C_p = pressure coefficient based on freestream static and dynamic pressures, $(p - p_0)/(\frac{1}{2}\rho U_0^2)$
C_y = sectional side-force coefficient, $\int C_p \sin\theta \, d\theta$
C_μ = forcing coefficient, $u^2 s_j / U_0^2 S$
D = maximum diameter of the forebody model
D_l = local diameter of the forebody model
p_0 = freestream static pressure
S = forebody model base area, $\pi D^2/4$
s_j = total area of the control ports
U_0 = freestream velocity
u = rms velocity through the control ports

Introduction

IT has been known for many years that slender bodies of revolution placed at high angles of attack produce a system of steady asymmetric vortices.[1] The vortex system induces an asymmetric pressure distribution on the surface of the forebody. Integration of the pressure distribution over the surface yields a net side force. Under some flight conditions, this side force can be as large as the normal force acting on the body.

Small geometric imperfections in the cone tip appear to be responsible for the development of the asymmetric vortices. As a result, the direction of the side force (yaw left or right) is not predictable. Numerical simulations by Degani[2] for the flow around a tangent-ogive forebody model at $\alpha = 40$ deg have shown that the vortices develop in an asymmetric pattern only when a small geometrical disturbance is added at the tip. Lamont[3] and Zilliac et al.[4] performed roll angle experiments with tangent-ogive forebody models at high angles of attack. For these experiments, the side force acting on the model varied with roll angle, clearly indicating a correlation between the vortex configuration and the position of the geometric asymmetry. Similar results have been obtained by Bridges and Hornung[5] with an elliptic cone and by Moskovitz[6] using small beads placed at different circumferential locations around the model tip. The implication of these results is that control of the flow asymmetry is possible by changes in the tip geometry.

The large side forces and yawing moments produced by the asymmetric forebody vortices can affect the yaw control characteristics of an aircraft and limit the maneuverability. At high angles of attack, the forebody vortices interact with the wing and vertical tail surfaces. These interactions can lead to roll oscillations of the aircraft called wing rock. Furthermore, the large side forces created by the asymmetric vortices can generate a torque resulting in the rotation of the vehicle about its center of gravity, which is known as coning motion. The coning motion of the body has been studied extensively by Ericsson and Reding[7] and Yoshinaga et al.[8]

Because of the importance of forebody vortex management, a variety of different passive and active flow control techniques have been devised. Passive control techniques typically use nose strakes to fix the flow separation lines, which forces the vortices into a symmetric configuration. Malcolm[9] discusses the effectiveness and limitations of passive control techniques. Active control methods include deployable strakes[10] and jet blowing.[11–13] Jet blowing has been demonstrated on several aircraft including the F-5, F-15, F-16, and X-29.

Considering the preceding remarks, one important research objective of the current investigation is to develop vortex control techniques that are capable of proportional control of the asymmetric forebody vortices. This type of control requires the capacity to change the vortex system between a yaw-left and yaw-right configuration to change the sign of the side force. In addition, the magnitude of the side force must be variable, indicating that the vortex configuration can be manipulated in a continuous manner. Effective control methods should be accomplished with very low input power levels for the technique to be attractive to the designer and should not adversely affect the performance of the aircraft. Ideally, the control techniques should not involve the use of external appendages such as nose strakes, which increase the drag on the flight vehicle. A potential benefit of proportional control is that the side force and yawing moment could be used to enhance the maneuverability of the aircraft.

The unsteady bleed technique is used for the experiments to control the development of the asymmetric forebody vortices. The basic premise of proportional control with the unsteady bleed technique is that controlling the initial flow disturbance at the tip can modify the configuration of the forebody vortices. The interaction of the unsteady bleed with the external flow produces a highly localized low-pressure disturbance in the mean flow with variable amplitude that dominates the built-in geometric asymmetry of the cone and controls the formation of the tip vortices. In addition to its role as an actuator, the unsteady bleed technique enables the investigation of the important flow physics by studying the response of the flow to a controlled input. In particular, it will be shown by use of the controlled input that a spatial instability may be responsible for the growth of the vortex asymmetry along the axis of the forebody model. Therefore, a second objective of the current research is to provide experimental evidence of the spatial instability. The fundamental nature of the instability will also be examined as the angle of attack is varied.

Received Dec. 5, 1997; revision received July 1, 1998; accepted for publication July 2, 1998.

*Postdoctoral Research Assistant, Department of Mechanical and Aerospace Engineering, Fluid Dynamics Research Center. Member AIAA.

†Professor, Department of Mechanical and Aerospace Engineering, Fluid Dynamics Research Center. Associate Fellow AIAA.

Experimental Configuration

Wind-Tunnel Facility

The experiments were conducted in a low-speed, open-return wind tunnel at the Fluid Dynamics Research Center of the Illinois Institute of Technology. The test section of the wind tunnel was 1.83 m long × 0.41 m wide × 0.61 m high (72 × 16 × 24 in.). The freestream turbulence level in the test section was less than 0.25%. A mounting sting inserted through the ceiling of the test section supported the forebody model in the wind tunnel and allowed the angle of attack to be varied from 0 to 90 deg.

Flow-visualization studies used two parallel smoke wires placed approximately 0.6 m (24 in.) upstream of the model. The two wires were adjusted so that the smoke entered the shear layer on both sides of the model. In this way, the two asymmetric vortices were evenly illuminated. By using one smoke wire at a time, independent flow visualizations of each vortex were obtained. Under some conditions, the wakes from the smoke wires created enough of a disturbance to change the vortex configuration. Therefore, the sectional side-force coefficient was constantly monitored to ensure repeatability. Either a strobe light or a laser sheet illuminated the smoke particles entrained by the vortices. The strobe light was placed underneath the test section floor, with the camera located off to the side. The strobe light visualizations gave a view of the entire flowfield. To view the flow locally, laser sheet flow visualizations were done using a 20-W copper vapor laser. The laser sheet intersected the axis of the model at right angles. The camera was aligned with a view looking along the model axis.

Quantitative velocity measurements were made using a two-component laser velocimeter operated in backscatter mode. The system employed a 5-W argon-ion laser mounted on a milling machine for accurate positioning. A six-jet atomizer using a 50:50 mixture of glycerin and water generated seeding particles. A pair of counters was used for signal processing.

The coordinate system defined for the velocity measurements is shown in Fig. 1. The origin of the coordinate system was located at the tip of the model. The z axis was aligned with the model centerline. Both the x axis and the y axis were perpendicular to the z axis and together formed a right-handed coordinate system. The laser Doppler velocimetry (LDV) system measured the velocity components parallel to the x axis (u component) and the z axis (w component). These measurements were made in the x–y plane at different axial locations. The sectional side-force coefficient was continuously monitored during the measurements to ensure that the seeding did not change the vortex configuration.

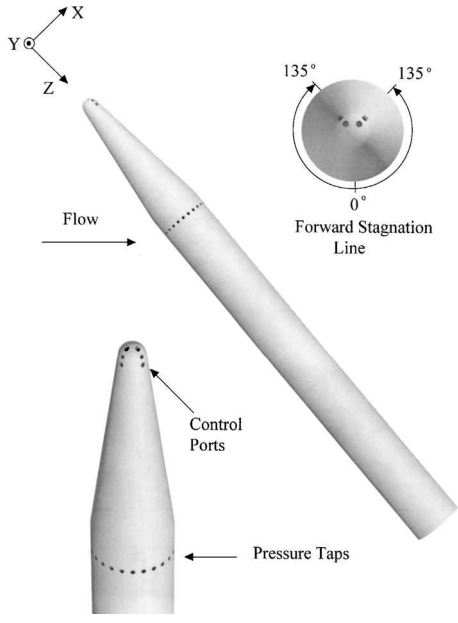

Fig. 1 Forebody model with a conical nose and rounded tip.

Forebody Model Configuration and Instrumentation

The forebody model designed for the experiments is shown in Fig. 1 with auxiliary views of the cone. The forebody model had a diameter of 2.86 cm (1.125 in.) and a fineness ratio of 10.7. The tip of the cone was rounded with a 0.476-cm (0.1875-in.) radius of curvature. The control ports consisted of small holes of diameter 1.6 mm (0.0625 in.) drilled into each side of the cone tip and located at ±135 deg from the forward stagnation line. Each set of holes was connected to a separate internal tube, so that each set could be independently activated. An additional 24 holes of diameter 1.6 mm (0.0625 in.) were drilled in 15-deg increments around the azimuth of the cylinder at a Z/D of 3.04. The pressure taps were connected through a rotary scanner to a differential pressure transducer. The main purpose of the pressure taps was to detect changes in the configuration of the forebody vortices. For each of the 24 azimuthal positions, a time-averaged pressure coefficient was calculated. The sectional side-force coefficient was computed from the C_p values by integrating the pressure distribution. The experimental accuracy of the C_p and C_y measurements was estimated to be ±0.03 and ±0.05, respectively.

The unsteady bleed apparatus consisted of two diaphragm-type chambers scavenged from a pair of small aquarium pumps. The rubber chambers were driven by a vibration exciter at a forcing frequency of 60 Hz. A 60-W power amplifier that received input from a function generator powered the vibration exciter. The forcing amplitude was measured with a pressure transducer connected to the control port tubes. The flow rate through each control port tube was regulated by a needle valve. Because the chamber valves were blocked, the only openings in the system were the control ports. Thus, there was no net mass added to the flow on average over a forcing cycle. During the first part of the cycle, air was pumped out of the forcing holes. The forcing holes behaved like freejets, and the pressure at the exit plane of the forcing holes was nearly atmospheric. During the second half of the cycle, the same amount of air was suctioned back into the system. The forcing holes behaved like sinks, and the exit pressure dropped below atmospheric. The unsteady bleed created a disturbance that altered the flow at the tip by the low-pressure region around the exit and through momentum addition to the flow.

The amplitude of the forcing was expressed as a nondimensional forcing coefficient in terms of a momentum flux ratio. The forcing coefficient C_μ physically represents the ratio of the momentum flux from the control ports to the incoming momentum that the model experiences. Positive forcing coefficients denote forcing through the control ports on the left-hand side of the model ($-y$ axis), whereas negative forcing coefficients indicate forcing on the right-hand side ($+y$ axis). The calculation of the forcing coefficient requires knowledge of the velocity at the exit plane of the control ports. A hot-wire probe was used to determine the rms exit velocities, which were related to the line pressures in the control port tubes.

Results

The results presented focus on two angles of attack, $\alpha = 45$ and 55 deg, because initial experiments with the forebody model indicated that significant differences in vortex behavior occurred in this range. Similarly, Zilliac et al.[4] demonstrated that the flow became bistable in this range. The yaw angle of the model was fixed at 0 deg, and the Reynolds number based on the freestream velocity and cylinder diameter was 6.3×10^3.

Forebody Vortex Behavior

The effect of forcing on the sectional side-force coefficient is shown in Fig. 2 for $\alpha = 45$ deg. The filled circle indicates the side force ($C_y = -0.51$) that occurs without forcing, resulting from the built-in geometric asymmetry of the model. When the unsteady bleed was activated on the same side as the primary vortex ($-y$ axis), the sectional side-force coefficient initially increased. The side-force coefficient continued to increase as the forcing level was increased until it saturated at $C_y = 0.60$ with $C_\mu = 0.004$. It was possible to achieve intermediate values of the side-force coefficient due to the continuous variation in the vortex configuration. Any additional increases in the forcing amplitude beyond the saturation point did

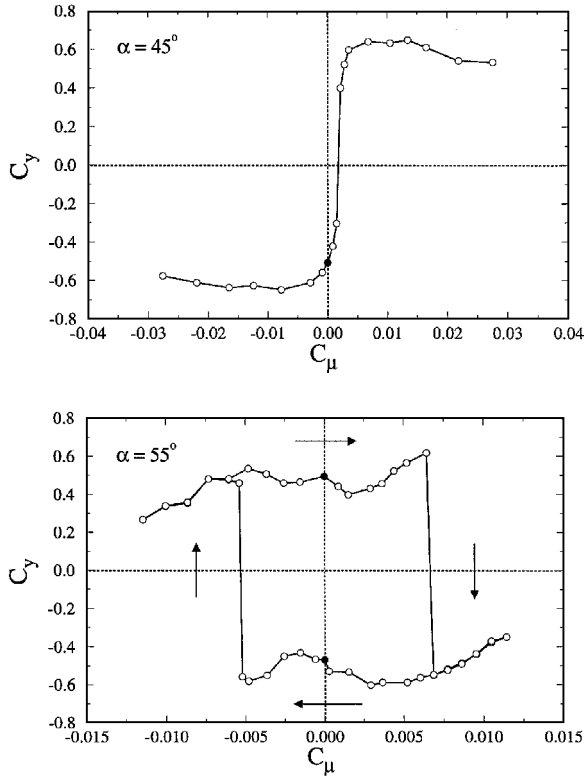

Fig. 2 Effect of forcing on the sectional side-force coefficient at $\alpha = 45$ and 55 deg.

not change the vortex configuration but did cause a slight reduction in the side-force coefficient. Activation of the control on the side opposite to the primary vortex ($+y$ axis) resulted in a decrease in C_y to -0.61 at $C_\mu = -0.003$. Further increases in the forcing amplitude caused a small reduction in the magnitude of C_y from the saturated value. It is important to note that the vortex system always returned to the original unforced configuration after the control was turned off on either side. These characteristics define the continuous behavior of the vortex system.

The forebody vortices displayed a fundamentally different behavior when the angle of attack was increased to $\alpha = 55$ deg, as shown in Fig. 2. The value of the side-force coefficient for the original state of the vortex system was $C_y = 0.49$, which corresponds to the upper filled symbol in the figure. For positive forcing coefficients, a transition point occurred at $C_\mu = 0.007$, where the vortices switched rapidly to the mirror image of their original configuration with $C_y = -0.55$. No intermediate states could be attained with the forcing system. Increasing the forcing amplitude beyond the transition point did not cause any major changes in the vortex configuration. Most importantly, the vortices did not return to their original configuration when the unsteady bleed was turned off. Instead, the side-force coefficient remained negative, with a value equal to -0.47 (lower filled symbol). This behavior of the vortex system is clear evidence of bistable states, where bistable is defined as the existence of two stable states of the flow in the absence of external perturbations.

A similar response of the vortex system was found for negative forcing coefficients. In this case, the vortex configuration switched at a transition forcing coefficient of $C_\mu = -0.005$. Once again, no intermediate values of C_y were achievable with the forcing system. Turning off the unsteady bleed recovered the original state of the flowfield. The combined positive and negative forcing formed a hysteresis loop in the C_y vs C_μ plot. The arrows in Fig. 2 show the path around the hysteresis loop.

Three different configurations of the vortex system were studied in detail at $\alpha = 45$ deg, including the unforced case (yaw right), the symmetric case (zero yaw), and the antisymmetric case (yaw left). The data for the unforced vortex configuration are shown in Fig. 3, where $C_y = -0.47$. Figure 3a consists of flow-visualization photographs of the forebody wake viewed from two distinct perspectives. The strobe light visualizations show side views of the forebody wake. The flowfield on the side of the model closest to the camera is visualized in the near-side photograph ($+y$ axis). The far-side photograph ($-y$ axis) is a visualization of the flowfield on the side of the model farthest from the camera. The pressure tap tubing is evident in the lower-right-hand portion of each photograph. The sides of the model are also labeled in the laser sheet visualization. The laser sheet visualization presents an axial view of the forebody wake. The laser sheet intersected the model axis at a Z/D of 3.04, which corresponded to the axial location of the pressure taps. The flow-visualization photographs for the unforced case clearly show that the vortices were asymmetric, as suggested by the nonzero value of C_y.

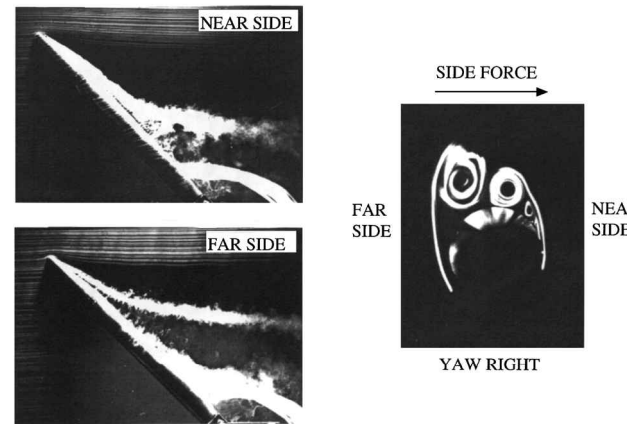

Fig. 3a Smoke wire flow-visualization photographs of the near- and far-side vortices for the unforced asymmetric case (yaw right).

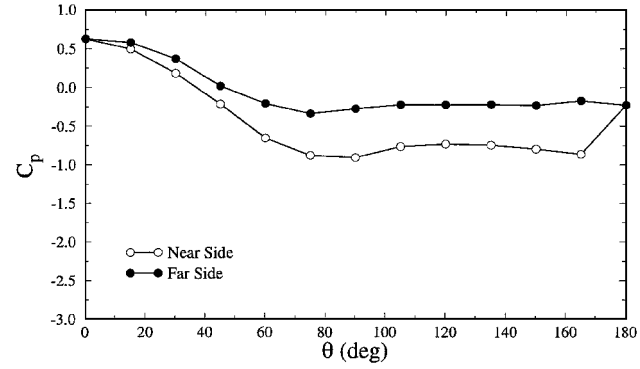

Fig. 3b Pressure distribution for the unforced asymmetric case (yaw right).

The pressure distribution for the unforced vortex configuration is presented in Fig. 3b. The value of the azimuthal angle θ at the forward stagnation point is 0 deg and increases to 180 deg at the back of the cylinder. The azimuthal angle is positive for both the near and far sides, so that the pressure distributions on the two sides may be easily compared. The pressure data show that the higher pressures occurred on the far side of the model (filled circles). The high-pressure region created a side force that acted to the right, as indicated by the arrow in Fig. 3a.

The near symmetric vortex configuration ($C_y = 0.01$) shown in Fig. 4 was attained by applying the unsteady bleed through the far-side control ports with $C_\mu = 0.002$. The symmetric nature of the vortices can be seen in both the strobe light and laser sheet flow visualizations. The pressure distributions on the near and far sides were almost identical, resulting in a side force that was approximately zero. Thus, the vortices in the symmetric state are not capable of yawing the model to the left or right.

When the control was activated on the far side with $C_\mu = 0.006$, the vortex system became asymmetric once again. The vortex configuration, however, was the reverse of the unforced arrangement with $C_y = 0.47$, as shown in Fig. 5. It is evident from the flow-visualization photographs that the vortex configuration was a mirror image of the configuration for the unforced case. The vortex

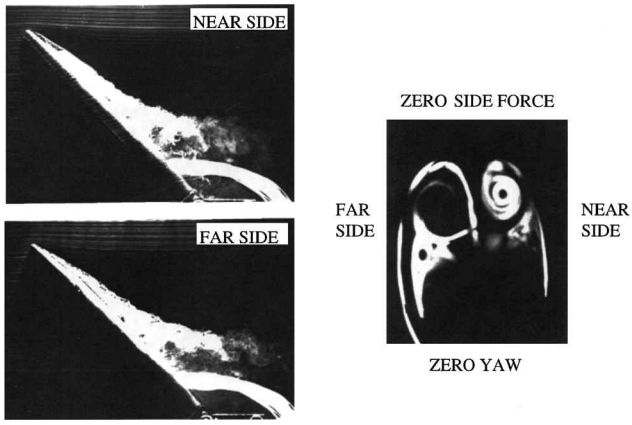

Fig. 4a Smoke wire flow-visualization photographs of the near- and far-side vortices for the symmetric case (zero yaw) achieved with forcing.

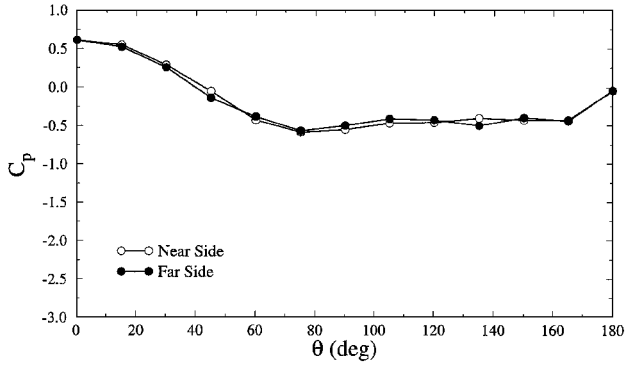

Fig. 4b Pressure distribution for the symmetric case (zero yaw) achieved with forcing.

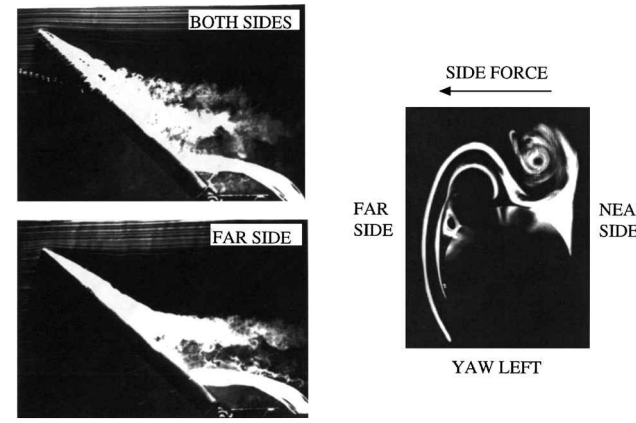

Fig. 5a Smoke wire flow-visualization photographs of the near- and far-side vortices for the antisymmetric case (yaw left) achieved with forcing.

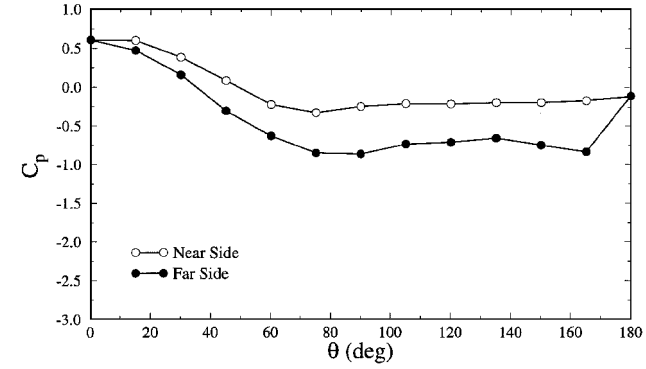

Fig. 5b Pressure distribution for the antisymmetric case (yaw left) achieved with forcing.

asymmetry is reflected in the pressure distribution, which shows that the higher pressures occurred on the near side of the model (open circles). The side force acted to the left, as shown by the arrow in Fig. 5a.

Spatial Instability Characteristics

It is generally agreed that the vortex asymmetry originates in the tip region of the forebody model. Despite careful machining of the forebody model, the cone tip always contains small geometric imperfections. These small imperfections are referred to as the geometric asymmetry of the cone, which produce the initial flow disturbance in the tip region. The development of the vortex asymmetry is due to the amplification of the initial tip asymmetry by a spatial instability in the forebody wake. Experimental evidence that supports the spatial instability concept is presented in this section.

One important aspect of the instability analysis is the measurement of the base flow state defined for the forebody wake as the state of the vortex system in the absence of any geometric asymmetry. Without the geometric asymmetry, the cone tip would be perfectly axisymmetric, and the vortices would be arranged in the symmetric configuration. Consequently, the symmetric state of the vortex system is taken as the base flow state for the instability analysis. Note that this definition of the base flow state is not accepted by all researchers.[14]

The symmetric state was attained experimentally by balancing the geometric asymmetry with a controlled disturbance from the unsteady bleed port. However, the forced flowfield may be different from the perfectly symmetric case if the forcing changes the mean velocity field. To check whether the forcing amplitude was large enough to distort the base velocity profile, several different forcing amplitudes were used. Mean and rms velocity profiles are plotted in Fig. 6 for $\alpha = 45$ deg. The symmetric state was first reached by applying the unsteady bleed through the far-side control ports with $C_\mu = 0.002$ (circles). Activating the control on the near side with $C_\mu = -0.005$ caused the vortex configuration to become asymmetric once again. Symmetry was restored by increasing the forcing amplitude on the far side to $C_\mu = 0.006$ (squares). This process of progressively increasing the forcing amplitude on both sides of the model was continued until a noticeable distortion in the velocity profiles occurred (asterisks). At the highest levels of forcing, the nonlinear effects of the unsteady bleed have become significant. However, at lower forcing amplitudes, the velocity profiles are not influenced by the nonlinearity of the control. Therefore, it is

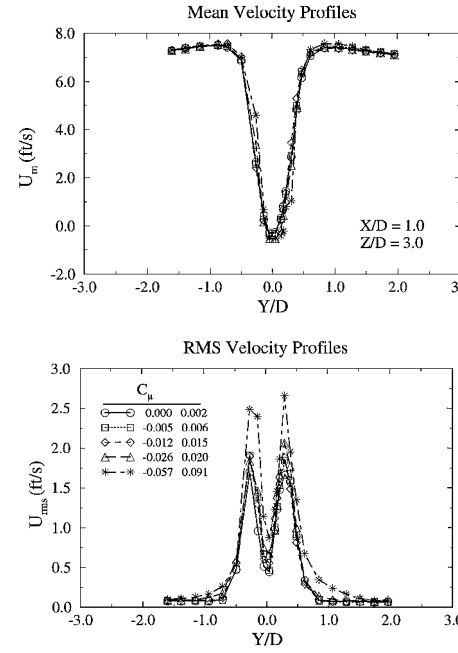

Fig. 6 Mean and rms velocity profiles for the symmetric case representing the base flow state.

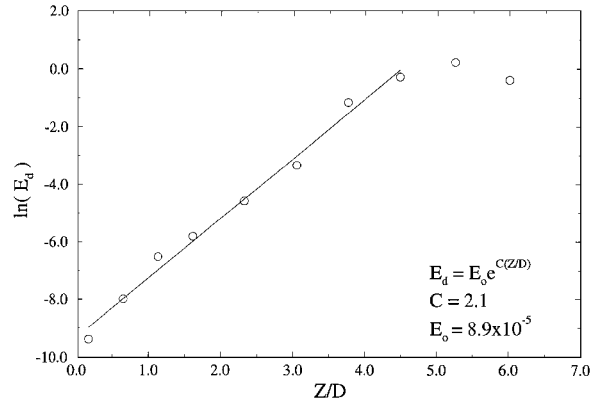

Fig. 7 Disturbance energy growth along the axis of the model.

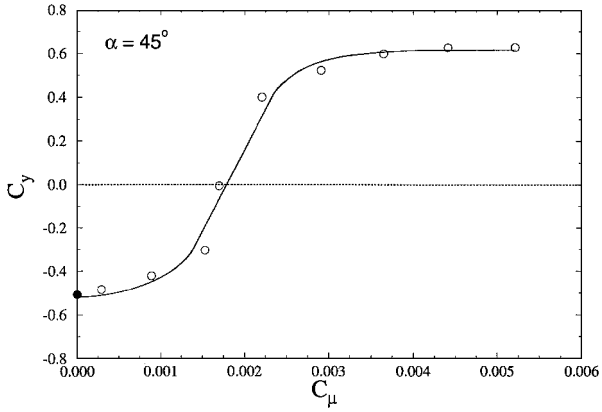

Fig. 8 Effect of forcing on C_y at $\alpha = 45$ deg, showing a linear region.

concluded that forcing at the low level of $C_\mu = 0.002$ produces a symmetric velocity profile equivalent to the base flow state.

The difference between the unforced and symmetric velocity profiles is a measure of the disturbance amplitude at a specific axial location. The disturbance amplitude refers to a steady distortion of the mean flow. The size of the spatially growing disturbance at a particular axial position can be quantified by defining a disturbance energy as follows:

$$E_d = \int_{-l/2}^{l/2} \frac{(U_a - U_s)^2}{U_0^2} \, \mathrm{d}\left(\frac{Y}{D}\right)$$

where U_a is the asymmetric mean velocity and U_s is the symmetric mean velocity. The quantity l represents the range of the velocity measurements in the y direction. The growth of the disturbance energy is plotted on semilog coordinates in Fig. 7. The data indicate exponential spatial growth from the tip of the model until $Z/D = 4.5$, at which point the disturbance energy saturates. A least-squares curve fitted to the experimental data of the form $E_d = E_0 \exp(CZ/D)$ reveals that the spatial growth rate $C = 2.1$ and the initial disturbance at the tip $E_0 = 8.9 \times 10^{-5}$. The initial disturbance energy at the tip is five orders of magnitude less than the disturbance energy at saturation.

The growth mechanism can be explored further by examining the data shown in Fig. 8, which shows the effect of forcing on C_y at $\alpha = 45$ deg for control applied only on the same side as the primary vortex ($-y$ axis). The curve fitted to the data indicates a region where a linear relationship exists between the input C_μ and the output C_y. The linear region is centered about the symmetric vortex configuration ($C_y = 0$) and extends to approximately $C_y = \pm 0.30$.

When the forcing is applied to the tip region, it takes a finite amount of time before the flow downstream of the tip responds. The time delay t_d between the application of the control and the response of the flow is shown in Fig. 9 for $\alpha = 45$ and 55 deg. The delay time was measured at $\alpha = 45$ deg with a hot-wire probe located at $X/D_l = 0.5$, $Y/D_l = -0.4$. For 55-deg angle of attack, LDV measurements were acquired at $X/D_l = 0.5$, $Y/D_l = -0.5$.

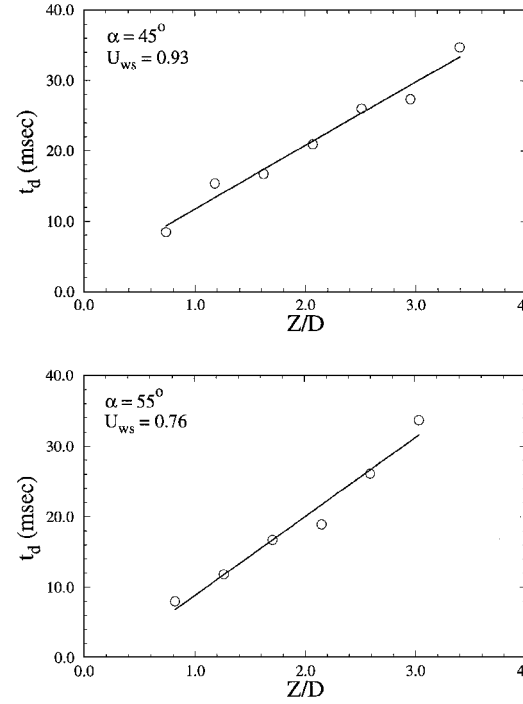

Fig. 9 Disturbance propagation speed along the axis of the model at $\alpha = 45$ and 55 deg.

Figure 9 shows that the delay increased linearly with distance from the tip, suggesting a constant wave speed. The wave propagation speed is the speed at which the disturbance travels through the forebody wake. The slopes of the lines drawn in Fig. 9 can be used to determine the wave propagation speeds. The wave propagation speeds normalized by freestream velocity U_{ws} at $\alpha = 45$ and 55 deg were calculated to be 0.93 and 0.76, respectively.

Discussion

Mechanism of Vortex Asymmetry

Two different mechanisms have been proposed that attempt to explain the development of the vortex asymmetry in the forebody wake. The first mechanism is based on the idea that the wake behaves like a spatial instability.[2] The second mechanism used to explain the vortex asymmetry focuses on the asymmetric separation points of the boundary layers on each side of the model, as described by Ericsson.[15] The spatial instability mechanism will be explored in further detail in this section.

The disturbance energy measurements provide evidence that a spatial instability of the forebody wake is responsible for the development of the vortex asymmetry, as suggested by Degani.[2] The data shown in Fig. 7 clearly indicate an exponential growth of the disturbance energy up to the nonlinear saturation point, which is consistent with a spatial type of flow instability. The growth of the vortex asymmetry with axial distance demonstrates that the symmetric base flow state is unstable to small disturbances at the model tip. Further evidence of a linear growth mechanism is presented in Fig. 8, where a region of linearity exists between the input C_μ and the output C_y. Thus, the spatial instability characteristics of the forebody wake play an important role in the development of the vortex asymmetry.

The development of the forebody flow asymmetry appears to be an inherently inviscid process. Marconi[16] solved the Euler equations numerically for the flow around slender right circular cones in a supersonic stream. The computations featured fixed separation points that were symmetrically located on the cone surface. Marconi found that both a symmetric and an asymmetric solution existed when $\alpha > 2.3\theta_c$, where θ_c is the cone half-angle. In the numerical simulations, the asymmetric solution was found to be stable and the symmetric solution unstable. The flow returned to an asymmetric state when the symmetry was not enforced. These asymmetric solutions seem to indicate that the development of the vortex asymmetry is inviscid in nature. Furthermore, asymmetric solutions of the Euler equations could be obtained with symmetric separation points.

This result implies that asymmetric separation is not necessarily a prerequisite for vortex asymmetry but rather a consequence of the vortex asymmetry due to an inviscid/viscid interaction. An example of this type of interaction is the pressure feedback from the forebody vortices to the tip in the case of global instability of the wake. The pressure feedback locks in the vortex configuration and causes the separation points to be asymmetric.

The initial flow disturbance produced by the geometric asymmetry of the cone is amplified by the spatial instability of the forebody wake. Note that only a very small geometric asymmetry or flow disturbance at the tip is necessary. At $\alpha = 45$ deg and $Re = 6.3 \times 10^3$, the measurements show that the initial disturbance energy at the tip was on the order of 10^{-5}, which is comparable to those found experimentally for the forcing coefficient. Typical orders of magnitude for the forcing coefficient range from 10^{-7} for steady suction[17] to 10^{-3} for unsteady bleed.

The concept of a spatial instability is a useful framework to explain how the initial tip asymmetry can be exploited to control the flow with very low levels of input power. By controlling the initial flow disturbance at the model tip, the asymmetry of the flowfield and the resulting side force can be modified. For example, the flow can be made symmetric and the side force eliminated by balancing the geometric asymmetry with a controlled disturbance produced by suction, blowing, or unsteady bleed. The controlled disturbance introduced at the tip effectively alters the net geometric asymmetry of the cone. Control of the side force can be accomplished with low forcing amplitudes and input power levels due to the amplification of the initial flow disturbance by the spatial instability. A system gain can be defined as the ratio of the side-force thrust power output to the actuator power input.[18] As a result of the spatial instability characteristics of the forebody wake, the system gain is on the order of 10^8 at a Reynolds number of 3×10^4.

The response of the vortex system shown in Fig. 9 amounts to a wave propagation speed through the wake. The controlled disturbance placed into the flow near the tip propagates downstream along the axis of the model. As a result, it takes a finite time for the flow downstream to respond to changes in the initial flow conditions at the tip. From a control systems perspective, a time delay exists between the application of the input and the response of the system.

Forebody Vortex Behavior

The results at $\alpha = 45$ deg show that the behavior of the vortex system is consistent with a convective instability. At this angle of attack, the vortex system responds to controlled disturbances in proportion to the amplitude of the disturbance. In addition, when the disturbance is removed, the flow returns to its unforced state. Degani[2] reached a similar conclusion based on numerical computations of the flow around a tangent-ogive forebody model. Because of the convective nature of the instability, a continuous change in the position of the vortices can be achieved, and proportional control with relatively low forcing amplitudes is possible.

The behavior of the vortex system at $\alpha = 55$ deg is indicative of a global type of instability. This vortex system behavior is clear evidence of bistable states, where bistable is defined as the existence of two stable states of the flow in the absence of any external disturbances (not including the geometric asymmetry). Pressure feedback from the vortices to the model tip induces an initial flow disturbance that can be greater than the disturbance produced by the geometric asymmetry. The self-induced asymmetry can lock in the vortex configuration. The vortices switch to the opposite configuration only when the forcing is able to overcome the feedback disturbance.

In addition to the angle of attack, it has been shown that the vortex system behavior is also dependent on the Reynolds number. Bernhardt and Williams[17] conducted experiments on the forebody model described in this paper for $6.2 \times 10^3 < Re < 3 \times 10^4$ at $\alpha = 55$ deg. As the Reynolds number was increased, the response of the vortex system changed from a bistable to a two-state to a continuous behavior. This change in the vortex system response corresponded to a transition from a global to a convective type of flow instability.

Conclusions

The mean velocity profiles measured behind the forebody model clearly show the exponential growth of a disturbance in the wake. This exponential growth is consistent with a spatial type of flow instability and indicates that the symmetric base flow state is unstable to small disturbances at the tip. Thus, the spatial instability characteristics of the forebody wake are responsible for the growth and development of the vortex asymmetry along the model axis. The initial flow disturbance at the tip is provided by the geometric asymmetry of the cone. The initial flow disturbance is amplified along the model axis by the spatial instability.

The type of spatial instability governing the flow determines the behavior of the vortex system. For a given model geometry, the nature of the instability depends on the angle of attack and the Reynolds number. The continuous response of the vortex system to forcing found at $\alpha = 45$ deg is consistent with a convective type of instability. Therefore, proportional control of the side force is possible for the continuous behavior. For the bistable behavior found at $\alpha = 55$ deg, the forebody wake shows characteristics similar to a global type of instability. Pressure feedback from the vortices induces a disturbance in the flow at the tip that can dominate the geometric asymmetry. The self-induced asymmetry can lock in the vortices and leads to two stable vortex configurations. Proportional control of the side force does not seem possible under these conditions for the bistable behavior.

However, it is also important to recognize that the fundamental nature of the spatial instability can change with the Reynolds number. Sectional side-force measurements show the change from a bistable to a two-state to a continuous behavior as the Reynolds number is increased. This change in the vortex system behavior corresponds to a transition from a global to a convective type of instability. Consequently, it seems reasonable that proportional control of the side force can be achieved at high Reynolds numbers.

It is fortunate that the flow around the forebody model is governed by a spatial instability. The amplification of small initial disturbances in the tip region by the spatial instability leads to a very large system gain. Therefore, the most effective control of the vortex configuration and the side force can be achieved by placing the flow actuators near the tip of the forebody model. By exploiting the spatial instability in this manner, control of the forebody vortices can be accomplished with very low forcing amplitudes and input power levels. Application of the control at the tip of the model changes the initial flow disturbance. As a result, the vortex configuration is modified along with the pressure distribution on the surface of the model. Control of the side force can be accomplished by this means.

The vortex system response to the control input applied at the model tip is characterized by a time delay. Changes in the initial flow conditions are propagated along the model axis at a fixed wave speed. Therefore, it takes a finite amount of time for the side force to develop on the forebody model after the control has been applied at the tip. The time delay is an important quantity because it determines how rapidly the side force can be changed on the forebody model.

Acknowledgments

This investigation has been conducted with the support of the Air Force Office of Scientific Research under Contract F49620-86-C-033 monitored by Daniel Fant and James McMichael. The assistance of Jaime Arenas and Andrew Barrett is greatly appreciated.

References

[1] Thomson, K. D., and Morrison, D. F., "The Spacing, Position and Strength of Vortices in the Wake of Slender Cylindrical Bodies at Large Incidence," *Journal of Fluid Mechanics*, Vol. 50, No. 4, 1971, pp. 751–783.

[2] Degani, D., "Numerical Investigation of the Origin of Vortex Asymmetry," AIAA Paper 90-0593, Jan. 1990.

[3] Lamont, P. J., "Pressures Around an Inclined Ogive Cylinder with Laminar, Transitional, or Turbulent Separation," *AIAA Journal*, Vol. 20, No. 11, 1982, pp. 1492–1499.

[4] Zilliac, G., Degani, D., and Tobak, M., "Asymmetric Vortices on a Slender Body of Revolution," AIAA Paper 90-0388, Jan. 1990.

[5] Bridges, D. H., and Hornung, H. G., "Elliptic Tip Effects on the Vortex Wake of an Axisymmetric Body at Incidence," *AIAA Journal*, Vol. 32, No. 7, 1994, pp. 1437–1445.

[6] Moskovitz, C. A., "An Experimental Investigation of the Physical Mechanisms Controlling the Asymmetric Flow Past Slender Bodies at Large Angles of Attack," Ph.D. Thesis, Dept. of Mechanical and Aerospace Engineering, North Carolina State Univ., Raleigh, NC, June 1989.

[7]Ericsson, L. E., and Reding, J. P., "Dynamics of Forebody Flow Separation and Associated Vortices," *Journal of Aircraft*, Vol. 22, No. 4, 1985, pp. 329–335.

[8]Yoshinaga, T., Tate, A., and Inoue, K., "Coning Motion of Slender Bodies at High Angles of Attack in Low Speed Flow," AIAA Paper 81-1899, Aug. 1981.

[9]Malcolm, G. N., "Forebody Vortex Control: A Progress Review," AIAA Paper 93-3540, Aug. 1993.

[10]Rao, D. M., Moskovitz, C., and Murri, D. G., "Forebody Vortex Management for Yaw Control at High Angles of Attack," *Journal of Aircraft*, Vol. 24, No. 4, 1987, pp. 248–254.

[11]Rom, J., and Almosnino, D., "Studies of Non-Linear Aerodynamic Characteristics of Finned Slender Bodies at High Angles of Attack," Technion—Israel Inst. of Technology, TAE 349, Haifa, Israel, Nov. 1978.

[12]Skow, A. M., Moore, W. A., and Lorincz, D. J., "Forebody Vortex Blowing—A Novel Concept to Enhance the Departure/Spin Recovery Characteristics of Fighter Aircraft," CP-262, AGARD, May 1979.

[13]Roos, F. W., and Magness, C. L., "Bluntness and Blowing for Flowfield Asymmetry Control on Slender Forebodies," AIAA Paper 93-3409, Aug. 1993.

[14]Ericsson, L. E., "The Fickle Effect of Nose Microasymmetry on High-Alpha Aerodynamics," AIAA Paper 90-0067, Jan. 1990.

[15]Ericsson, L. E., "Sources of High Alpha Vortex Asymmetry at Zero Sideslip," *Journal of Aircraft*, Vol. 29, No. 6, 1992, pp. 1086–1090.

[16]Marconi, F., "Asymmetric Separated Flows About Sharp Cones in a Supersonic Stream," *Proceedings of the 11th International Conference on Numerical Methods in Fluid Dynamics* (Williamsburg, VA), Springer–Verlag, New York, 1988, pp. 395–402.

[17]Bernhardt, J., and Williams, D., "The Effect of Reynolds Number on Vortex Asymmetry About Slender Bodies," *Physics of Fluids A*, Vol. 5, No. 2, 1993, pp. 291–293.

[18]Bernhardt, J., and Williams, D., "The Effect of Reynolds Number on Control of Forebody Asymmetry by Suction and Bleed," AIAA Paper 93-3265, July 1993.

A. Plotkin
Associate Editor